

EFFECT OF WALL COMPLIANCE ON PERISTALTIC TRANSPORT OF A NEWTONIAN FLUID IN AN ASYMMETRIC CHANNEL

MOHAMED H. HAROUN

Received 19 January 2006; Revised 5 April 2006; Accepted 24 May 2006

Peristaltic transport of an incompressible viscous fluid in an asymmetric compliant channel is studied. The channel asymmetry is produced by choosing the peristaltic wave train on the walls to have different amplitudes and phases. The fluid-solid interaction problem is investigated by considering equations of motion of both the fluid and the deformable boundaries. The driving mechanism of the muscle is represented by assuming the channel walls to be compliant. The phenomenon of the “mean flow reversal” is discussed. The effect of wave amplitude ratio, width of the channel, phase difference, wall elastance, wall tension, and wall damping on mean-velocity and reversal flow has been investigated. The results reveal that the reversal flow occurs near the boundaries which is not possible in the elastic symmetric channel case.

Copyright © 2006 Mohamed H. Haroun. This is an open access article distributed under the Creative Commons Attribution License, which permits unrestricted use, distribution, and reproduction in any medium, provided the original work is properly cited.

1. Introduction

Peristaltic transport is a form of fluid transport induced by a progressive wave of area contraction or expansion along the length of a distensible tube containing fluid. In physiology, peristalsis is used by the body to propel or mix the contents of a tube as in ureter, gastrointestinal tract, bile duct, and other glandular ducts. Some worms use peristalsis as a means of locomotion. Roller and finger pumps using viscous fluids also operate on this principle. Peristalsis has been proposed as a mechanism for the transport of spermatozoa in vas deferens (Paufler and Foote [18]). Vas deferens is the duct which connects the ductus epididymidis to an ampulla. The mechanism of peristaltic transport has been exploited for industrial applications like sanitary fluid transport, blood pumps in heart lung machine, and transport of corrosive fluids where the contact of the fluid with the machinery parts is prohibited. The problem of the mechanism of peristaltic transport has attracted the attention of many investigators since the first investigation of Latham [12].

2 Effect of wall compliance on peristaltic transport

A number of analytical and experimental studies have been conducted to understand peristaltic action have appeared in [1, 3, 6, 7, 11, 13–15, 19, 25, 26]. Numerical techniques were used by Brown and Hung [2]; Takabatake and Ayukawa [23] for channel flow, and Takabatake et al. [24] for axisymmetric tube flow. A summary of most of the investigation reported up to the year 1984 has been presented by L. M. Srivastava and V. P. Srivastava [21]. The important contributions of the recent years are referenced by Srivastava and Saxena [20]. Recently, physiologists observed that the intrauterine fluid flow due to myometrial contractions is peristaltic-type motion and the myometrial contractions may occur in both symmetric and asymmetric direction (de Vries et al. [5]). Eytan and Elad [8] have developed a mathematical model of wall-induced peristaltic fluid flow in a two-dimensional channel with wave trains having a phase difference moving independently on the upper and lower walls to simulate intrauterine fluid motion in a sagittal cross-section of the uterus. Eytan et al. [9] have observed that the width of the sagittal cross-section of the uterine cavity increases towards the fundus, and the cavity is not fully occluded during the contractions. Mitra and Prasad [17] extended Fung and Yih [10] model and considered the two-dimensional analysis of peristaltic motion with flexible (elastic or viscoelastic) wall. L. M. Srivastava and V. P. Srivastava [22] extended the work of Mitra and Prasad [17] from single-phase Newtonian fluid analysis to a two-phase flow. The present study extends the two-dimensional analysis of peristaltic motion by (Mitra and Prasad [17] and Mishra and Rao [16]) to include a compliant asymmetric channel. The main purpose of the present study is to investigate the influence of compliant wall properties in peristaltic motion in a two-dimensional asymmetric channel which is different from the model used by Mitra and Prasad [17]. Also, the chief aim of the present study is to understand the dynamic interaction of fluid and solid inherent in peristalsis. Therefore, no attempt is made to discuss the origin of the source of energy or how a progressive wave may be imparted to the walls. The compliant wall is excited by the muscles whose tension will control its deformation. The action of these muscles will be governed by a set of equations in terms of variables which will be related to the compliant wall displacement. In the present analysis this driving mechanism of the muscle is assumed in the form of a sinusoidal wave of moderate amplitude imposed on the compliant walls of the channel. The channel asymmetry is produced by choosing the peristaltic wave train on the walls to have different amplitudes and phases. The equations of the motion for the fluid are solved taking into account the nonlinearity of these equations and the action of the walls. As the problem is complicated, it is solved by perturbation technique which is different from the method used by Mishra and Rao [16].

2. Basic equations and formulation of the problem

A viscous incompressible fluid of density ρ and kinematic viscosity ν flows in a two-dimensional asymmetric channel of width $d_1 + d_2$. The channel asymmetry is produced by choosing the peristaltic wave train on the walls to have different amplitudes and phases. The walls of the channel are flexible, considered as compliant walls (see Figure 2.1). The basic flow is taken parallel to the x -axis with the y -axis normal to the walls. Denoting the x and y velocity components of the fluid by u and v and the pressure by P , the equation

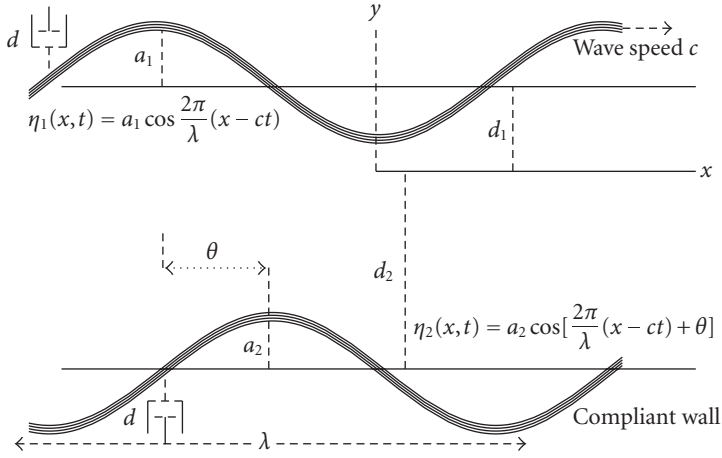


Figure 2.1. Geometry of the problem.

of continuity and the equations of motion are

$$\frac{\partial u}{\partial x} + \frac{\partial v}{\partial y} = 0, \quad (2.1)$$

$$\frac{\partial u}{\partial t} + u \frac{\partial u}{\partial x} + v \frac{\partial u}{\partial y} = -\frac{1}{\rho} \frac{\partial P}{\partial x} + \nu \nabla^2 u, \quad (2.2)$$

$$\frac{\partial v}{\partial t} + u \frac{\partial v}{\partial x} + v \frac{\partial v}{\partial y} = -\frac{1}{\rho} \frac{\partial P}{\partial y} + \nu \nabla^2 v.$$

We define the stream function $\psi(x, y, t)$ by

$$u = \frac{\partial \psi}{\partial y}, \quad v = -\frac{\partial \psi}{\partial x}. \quad (2.3)$$

Substituting (2.3) into (2.2) and eliminating the pressure, we get

$$\frac{\partial}{\partial t} \nabla^2 \psi + \psi_y \nabla^2 \psi_x - \psi_x \nabla^2 \psi_y = \nu \nabla^2 \nabla^2 \psi, \quad (2.4)$$

where ∇^2 denotes the Laplacian operator, and the subscripts indicate partial differentiation.

The compliant wall is modeled as spring-backed plate, it constrained to move only in the vertical direction. Let the vertical displacements of the upper and lower walls be η_1 and η_2 , respectively. Further, η_1 and η_2 are assumed to be in the form of a sinusoidal waves of different amplitudes and phases. Thus,

$$\eta_1 = a_1 \cos \frac{2\pi}{\lambda}(x-ct), \quad \eta_2 = a_2 \cos \left[\frac{2\pi}{\lambda}(x-ct) + \theta \right], \quad (2.5)$$

4 Effect of wall compliance on peristaltic transport

where a_1 and a_2 are the amplitudes of the waves, λ is the wave length, c is the wave speed, and θ is the phase difference which varies in the range $0 \leq \theta \leq \pi$. It should be noted that $\theta = 0$ corresponds to symmetric channel with waves out of phase, $\theta = \pi$ with waves in phase, and further a_1, a_2, d_1, d_2 , and θ satisfy the condition $a_1^2 + a_2^2 + 2a_1a_2 \cos \theta \leq (d_1 + d_2)^2$. The equation of motion of the compliant wall can be written as (Davies and Carpenter [4])

$$\left[m \frac{\partial^2}{\partial t^2} + d \frac{\partial}{\partial t} + B \frac{\partial^4}{\partial x^4} - T \frac{\partial^2}{\partial x^2} + K \right] \begin{Bmatrix} \eta_1 \\ \eta_2 \end{Bmatrix} = P - P_0, \quad (2.6)$$

where m is the plate mass per unit area, d is the wall damping coefficient, B is the flexural rigidity of the plate, T is the longitudinal tension per unit width, K is the spring stiffness, and P_0 is the pressure on the outside surface of the wall due to the tension in the muscles. This tension may be obtained through the constitutive relation of the muscles when the displacements are known. It is assumed that $P_0 = 0$ and the channel walls are inextensible so that only their lateral motions normal to the undeformed positions occur. The horizontal displacement will be assumed zero. Hence the boundary conditions for the fluid are

$$\begin{aligned} \psi_y = 0, \quad \psi_x = -\frac{\partial \eta_1}{\partial t} \quad \text{at } y = d_1 + \eta_1, \\ \psi_y = 0, \quad \psi_x = \frac{\partial \eta_2}{\partial t} \quad \text{at } y = -d_2 - \eta_2. \end{aligned} \quad (2.7)$$

Continuity of stresses requires that at the interfaces of the walls and the fluid P must be the same as that which acts on the fluid at $y = d_1 + \eta_1$ and $y = -d_2 - \eta_2$. The use of x -momentum equation leads to

$$\frac{\partial}{\partial x} \left[m \frac{\partial^2}{\partial t^2} + d \frac{\partial}{\partial t} + B \frac{\partial^4}{\partial x^4} - T \frac{\partial^2}{\partial x^2} + K \right] \begin{Bmatrix} \eta_1 \\ \eta_2 \end{Bmatrix} = \rho v \nabla^2 \psi_y - \rho (\psi_{yt} + \psi_y \psi_{yx} - \psi_x \psi_{yy}). \quad (2.8)$$

We introduce nondimensional variables and parameters as follows:

$$\begin{aligned} x^* = \frac{x}{d_1}, \quad y^* = \frac{y}{d_1}, \quad u^* = \frac{u}{c}, \quad v^* = \frac{v}{c}, \quad t^* = \frac{ct}{d_1}, \quad p^* = \frac{p}{\rho c^2}, \\ \eta_1^* = \frac{\eta_1}{d_1}, \quad \eta_2^* = \frac{\eta_2}{d_1}, \quad \psi^* = \frac{\psi}{cd_1}, \quad m^* = \frac{m}{\rho d_1}, \quad d^* = \frac{dd_1}{\rho v}, \\ B^* = \frac{B}{\rho d_1 v^2}, \quad T^* = \frac{Td_1}{\rho v^2}, \quad K^* = \frac{Kd_1^3}{\rho v^2}, \end{aligned} \quad (2.9)$$

$\epsilon = a_1/d_1$, $h = d_2/d_1$, $a = a_2/a_1$, wave number $\alpha = 2\pi d_1/\lambda$, and Reynolds number $R = cd_1/\nu$. Dropping the star over the symbols, (2.4)–(2.8) become

$$\frac{\partial}{\partial t} \nabla^2 \psi + \psi_y \nabla^2 \psi_x - \psi_x \nabla^2 \psi_y = \frac{1}{R} \nabla^4 \psi, \quad (2.10)$$

$$\eta_1 = \epsilon \text{Cos} \alpha(x - t), \quad \eta_2 = a\epsilon \text{Cos} [\alpha(x - t) + \theta], \quad (2.11)$$

$$\psi_y = 0, \quad \psi_x = -a\epsilon \text{Sin} \alpha(x - t) \quad \text{at } y = 1 + \eta_1, \quad (2.12)$$

$$\psi_y = 0, \quad \psi_x = a\alpha\epsilon \text{Sin} [\alpha(x - t) + \theta] \quad \text{at } y = -h - \eta_2, \quad (2.13)$$

$$\begin{aligned} \frac{\partial}{\partial x} \left[m \frac{\partial^2}{\partial t^2} + \frac{d}{R} \frac{\partial}{\partial t} + \frac{B}{R^2} \frac{\partial^4}{\partial x^4} - \frac{T}{R^2} \frac{\partial^2}{\partial x^2} + \frac{K}{R^2} \right] \begin{Bmatrix} \eta_1 \\ \eta_2 \end{Bmatrix} \\ = \frac{1}{R} \nabla^2 \psi_y - \psi_{yt} - \psi_y \psi_{yx} + \psi_x \psi_{yy} \quad \text{at } y = \begin{Bmatrix} 1 + \eta_1 \\ -h - \eta_2 \end{Bmatrix}. \end{aligned} \quad (2.14)$$

3. Method of solution

We obtain the solution for the stream function as a power series in terms of the small amplitude ratio (wave amplitude/channel half width) ϵ , by expanding ψ and $\partial p/\partial x$ in the form (see Fung and Yih [10])

$$\psi = \psi_0 + \epsilon \psi_1 + \epsilon^2 \psi_2 + \dots, \quad (3.1)$$

$$\left(\frac{\partial p}{\partial x} \right) = \left(\frac{\partial p}{\partial x} \right)_0 + \epsilon \left(\frac{\partial p}{\partial x} \right)_1 + \epsilon^2 \left(\frac{\partial p}{\partial x} \right)_2 + \dots \quad (3.2)$$

The first term on the right-hand side in (3.2) corresponds to the imposed pressure gradient and the other terms correspond to the peristaltic motion. Substituting (3.1) into (2.10), (2.12), (2.13), and (2.14) and collecting terms of like powers of ϵ , we obtain

$$\frac{\partial}{\partial t} \nabla^2 \psi_0 + \psi_{0y} \nabla^2 \psi_{0x} - \psi_{0x} \nabla^2 \psi_{0y} = \frac{1}{R} \nabla^4 \psi_0,$$

$$\psi_{0y} \begin{Bmatrix} 1 \\ -h \end{Bmatrix} = 0, \quad \psi_{0x} \begin{Bmatrix} 1 \\ -h \end{Bmatrix} = 0,$$

$$\frac{1}{R} \nabla^2 \psi_{0y} \begin{Bmatrix} 1 \\ -h \end{Bmatrix} - \psi_{0ty} \begin{Bmatrix} 1 \\ -h \end{Bmatrix} - \psi_{0y} \begin{Bmatrix} 1 \\ -h \end{Bmatrix} \psi_{0yx} \begin{Bmatrix} 1 \\ -h \end{Bmatrix} + \psi_{0x} \begin{Bmatrix} 1 \\ -h \end{Bmatrix} \psi_{0yy} \begin{Bmatrix} 1 \\ -h \end{Bmatrix} = 0,$$

$$\frac{\partial}{\partial t} \nabla^2 \psi_1 + \psi_{0y} \nabla^2 \psi_{1x} + \psi_{1y} \nabla^2 \psi_{0x} - \psi_{0x} \nabla^2 \psi_{1y} - \psi_{1x} \nabla^2 \psi_{0y} = \frac{1}{R} \nabla^4 \psi_1,$$

$$\psi_{1y} \begin{Bmatrix} 1 \\ -h \end{Bmatrix} \pm \begin{Bmatrix} \text{Cos} \alpha(x - t) \\ a \text{Cos} [\alpha(x - t) + \theta] \end{Bmatrix} \psi_{0yy} \begin{Bmatrix} 1 \\ -h \end{Bmatrix} = 0,$$

$$\psi_{1x} \begin{Bmatrix} 1 \\ -h \end{Bmatrix} \pm \begin{Bmatrix} \text{Cos} \alpha(x - t) \\ a \text{Cos} [\alpha(x - t) + \theta] \end{Bmatrix} \psi_{0xy} \begin{Bmatrix} 1 \\ -h \end{Bmatrix} = \pm \begin{Bmatrix} \alpha \text{Sin} \alpha(x - t) \\ a \alpha \text{Sin} [\alpha(x - t) + \theta] \end{Bmatrix},$$

6 Effect of wall compliance on peristaltic transport

$$\begin{aligned}
& \frac{\partial}{\partial x} \left[m \frac{\partial^2}{\partial t^2} + \frac{d}{R} \frac{\partial}{\partial t} + \frac{B}{R^2} \frac{\partial^4}{\partial x^4} - \frac{T}{R^2} \frac{\partial^2}{\partial x^2} + \frac{K}{R^2} \right] \left\{ \begin{array}{c} \text{Cos} \alpha(x-t) \\ a \text{Cos}[\alpha(x-t) + \theta] \end{array} \right\} \\
&= \frac{1}{R} \nabla^2 \psi_{1y} \left\{ \begin{array}{c} 1 \\ -h \end{array} \right\} - \psi_{1ty} \left\{ \begin{array}{c} 1 \\ -h \end{array} \right\} - \psi_{0y} \left\{ \begin{array}{c} 1 \\ -h \end{array} \right\} \psi_{1yx} \left\{ \begin{array}{c} 1 \\ -h \end{array} \right\} - \psi_{1y} \left\{ \begin{array}{c} 1 \\ -h \end{array} \right\} \psi_{0yx} \left\{ \begin{array}{c} 1 \\ -h \end{array} \right\} \\
&+ \psi_{0x} \left\{ \begin{array}{c} 1 \\ -h \end{array} \right\} \psi_{1yy} \left\{ \begin{array}{c} 1 \\ -h \end{array} \right\} + \psi_{1x} \left\{ \begin{array}{c} 1 \\ -h \end{array} \right\} \psi_{0yy} \left\{ \begin{array}{c} 1 \\ -h \end{array} \right\} \\
&\pm \left\{ \begin{array}{c} \text{Cos} \alpha(x-t) \\ a \text{Cos}[\alpha(x-t) + \theta] \end{array} \right\} \left[\frac{1}{R} \nabla^2 \psi_{0yy} \left\{ \begin{array}{c} 1 \\ -h \end{array} \right\} - \psi_{0tyy} \left\{ \begin{array}{c} 1 \\ -h \end{array} \right\} - \psi_{0y} \left\{ \begin{array}{c} 1 \\ -h \end{array} \right\} \psi_{0yyx} \left\{ \begin{array}{c} 1 \\ -h \end{array} \right\} \right. \\
&\quad \left. - \psi_{0yy} \left\{ \begin{array}{c} 1 \\ -h \end{array} \right\} \psi_{0yx} \left\{ \begin{array}{c} 1 \\ -h \end{array} \right\} + \psi_{0x} \left\{ \begin{array}{c} 1 \\ -h \end{array} \right\} \psi_{0yyy} \left\{ \begin{array}{c} 1 \\ -h \end{array} \right\} \right. \\
&\quad \left. + \psi_{0yx} \left\{ \begin{array}{c} 1 \\ -h \end{array} \right\} \psi_{0yy} \left\{ \begin{array}{c} 1 \\ -h \end{array} \right\} \right],
\end{aligned}$$

$$\frac{\partial}{\partial t} \nabla^2 \psi_2 + \psi_{0y} \nabla^2 \psi_{2x} + \psi_{1y} \nabla^2 \psi_{1x} + \psi_{2y} \nabla^2 \psi_{0x} - \psi_{0x} \nabla^2 \psi_{2y} - \psi_{1x} \nabla^2 \psi_{1y} - \psi_{2x} \nabla^2 \psi_{0y} = \frac{1}{R} \nabla^4 \psi_2,$$

$$\psi_{2y} \left\{ \begin{array}{c} 1 \\ -h \end{array} \right\} \pm \left\{ \begin{array}{c} \text{Cos} \alpha(x-t) \\ a \text{Cos}[\alpha(x-t) + \theta] \end{array} \right\} \psi_{1yy} \left\{ \begin{array}{c} 1 \\ -h \end{array} \right\} + \frac{1}{2} \left\{ \begin{array}{c} \text{Cos}^2 \alpha(x-t) \\ a^2 \text{Cos}^2[\alpha(x-t) + \theta] \end{array} \right\} \psi_{0yyy} \left\{ \begin{array}{c} 1 \\ -h \end{array} \right\} = 0,$$

$$\psi_{2x} \left\{ \begin{array}{c} 1 \\ -h \end{array} \right\} \pm \left\{ \begin{array}{c} \text{Cos} \alpha(x-t) \\ a \text{Cos}[\alpha(x-t) + \theta] \end{array} \right\} \psi_{1xy} \left\{ \begin{array}{c} 1 \\ -h \end{array} \right\} + \frac{1}{2} \left\{ \begin{array}{c} \text{Cos}^2 \alpha(x-t) \\ a^2 \text{Cos}^2[\alpha(x-t) + \theta] \end{array} \right\} \psi_{0xyy} \left\{ \begin{array}{c} 1 \\ -h \end{array} \right\} = 0,$$

$$\begin{aligned}
& \frac{1}{R} \nabla^2 \psi_{2y} \left\{ \begin{array}{c} 1 \\ -h \end{array} \right\} - \psi_{2ty} \left\{ \begin{array}{c} 1 \\ -h \end{array} \right\} - \psi_{0y} \left\{ \begin{array}{c} 1 \\ -h \end{array} \right\} \psi_{2yx} \left\{ \begin{array}{c} 1 \\ -h \end{array} \right\} \\
&\quad - \psi_{1y} \left\{ \begin{array}{c} 1 \\ -h \end{array} \right\} \psi_{1yx} \left\{ \begin{array}{c} 1 \\ -h \end{array} \right\} - \psi_{2y} \left\{ \begin{array}{c} 1 \\ -h \end{array} \right\} \psi_{0yx} \left\{ \begin{array}{c} 1 \\ -h \end{array} \right\} \\
&\quad + \psi_{0x} \left\{ \begin{array}{c} 1 \\ -h \end{array} \right\} \psi_{2yy} \left\{ \begin{array}{c} 1 \\ -h \end{array} \right\} + \psi_{1x} \left\{ \begin{array}{c} 1 \\ -h \end{array} \right\} \psi_{1yy} \left\{ \begin{array}{c} 1 \\ -h \end{array} \right\} + \psi_{2x} \left\{ \begin{array}{c} 1 \\ -h \end{array} \right\} \times \psi_{0yy} \left\{ \begin{array}{c} 1 \\ -h \end{array} \right\} \\
&\quad \pm \left\{ \begin{array}{c} \text{Cos} \alpha(x-t) \\ a \text{Cos}[\alpha(x-t) + \theta] \end{array} \right\} \left[\frac{1}{R} \nabla^2 \psi_{1yy} \left\{ \begin{array}{c} 1 \\ -h \end{array} \right\} - \psi_{1tyy} \left\{ \begin{array}{c} 1 \\ -h \end{array} \right\} - \psi_{0y} \left\{ \begin{array}{c} 1 \\ -h \end{array} \right\} \right. \\
&\quad \times \psi_{1yyx} \left\{ \begin{array}{c} 1 \\ -h \end{array} \right\} - \psi_{1y} \left\{ \begin{array}{c} 1 \\ -h \end{array} \right\} \psi_{0yyx} \left\{ \begin{array}{c} 1 \\ -h \end{array} \right\} \\
&\quad \left. - \psi_{0yy} \left\{ \begin{array}{c} 1 \\ -h \end{array} \right\} \psi_{1yx} \left\{ \begin{array}{c} 1 \\ -h \end{array} \right\} - \psi_{1yy} \left\{ \begin{array}{c} 1 \\ -h \end{array} \right\} \psi_{0yx} \left\{ \begin{array}{c} 1 \\ -h \end{array} \right\} \right. \\
&\quad \left. + \psi_{0x} \left\{ \begin{array}{c} 1 \\ -h \end{array} \right\} \psi_{1yyy} \left\{ \begin{array}{c} 1 \\ -h \end{array} \right\} + \psi_{1x} \left\{ \begin{array}{c} 1 \\ -h \end{array} \right\} \psi_{0yyy} \left\{ \begin{array}{c} 1 \\ -h \end{array} \right\} \right. \\
&\quad \left. + \psi_{0yx} \left\{ \begin{array}{c} 1 \\ -h \end{array} \right\} \psi_{1yy} \left\{ \begin{array}{c} 1 \\ -h \end{array} \right\} + \psi_{1yx} \left\{ \begin{array}{c} 1 \\ -h \end{array} \right\} \times \psi_{0yy} \left\{ \begin{array}{c} 1 \\ -h \end{array} \right\} \right]
\end{aligned}$$

$$\begin{aligned}
 & + \frac{1}{2} \left\{ \frac{\cos^2 \alpha(x-t)}{a^2 \cos^2[\alpha(x-t) + \theta]} \right\} \left[\frac{1}{R} \nabla^2 \psi_{0yyy} \left\{ \frac{1}{-h} \right\} - \psi_{0tyyy} \left\{ \frac{1}{-h} \right\} - \psi_{0y} \left\{ \frac{1}{-h} \right\} \right. \\
 & \quad \times \psi_{0yyyx} \left\{ \frac{1}{-h} \right\} - \psi_{0yy} \left\{ \frac{1}{-h} \right\} \psi_{0yyx} \left\{ \frac{1}{-h} \right\} \\
 & \quad - \psi_{0yyy} \left\{ \frac{1}{-h} \right\} \psi_{0yx} \left\{ \frac{1}{-h} \right\} + \psi_{0x} \left\{ \frac{1}{-h} \right\} \\
 & \quad \times \psi_{0yyy} \left\{ \frac{1}{-h} \right\} + \psi_{0yx} \left\{ \frac{1}{-h} \right\} \psi_{0yyy} \left\{ \frac{1}{-h} \right\} \\
 & \quad \left. + \psi_{0yyx} \left\{ \frac{1}{-h} \right\} \psi_{0yy} \left\{ \frac{1}{-h} \right\} \right] = 0.
 \end{aligned} \tag{3.3}$$

The first set of differential equations in ψ_0 , subject to the steady parallel flow under the effect of a constant pressure gradient in the x -direction, yields

$$\begin{aligned}
 \psi_0 &= K_0 \left[\frac{(h-1)(h^2 + 4h + 1)}{12} + hy - \frac{(h-1)}{2} y^2 - \frac{y^3}{3} \right], \\
 K_0 &= -\frac{R}{2} \left(\frac{dP}{dx} \right)_0.
 \end{aligned} \tag{3.4}$$

The second and third sets of differential equations in ψ_1 and ψ_2 with their corresponding boundary conditions are satisfied by

$$\begin{aligned}
 \psi_1(x, y, t) &= \frac{1}{2} (\phi_1(y) e^{i\alpha(x-t)} + \phi_1^*(y) e^{-i\alpha(x-t)}), \\
 \psi_2(x, y, t) &= \frac{1}{2} (\phi_{20}(y) + \phi_{22}(y) e^{2i\alpha(x-t)} + \phi_{22}^*(y) e^{-2i\alpha(x-t)}),
 \end{aligned} \tag{3.5}$$

where the asterisk denotes the complex conjugate. Substituting of (3.5) into the differential equations and their corresponding boundary conditions in ψ_1 and ψ_2 , we get

$$\left(\frac{d^2}{dy^2} - \alpha^2 + i\alpha R(1 - \psi'_0) \right) \left(\frac{d^2}{dy^2} - \alpha^2 \right) \phi_1(y) + i\alpha R \psi_0''' \phi_1(y) = 0, \tag{3.6}$$

$$\phi_1' \left\{ \frac{1}{-h} \right\} = \left\{ \frac{-1}{ae^{i\theta}} \right\} \psi_0'' \left\{ \frac{1}{-h} \right\}, \tag{3.7}$$

$$\phi_1''' \left\{ \frac{1}{-h} \right\} - \alpha(\alpha - iR) \phi_1' \left\{ \frac{1}{-h} \right\} + i\alpha \psi_0'' \left\{ \frac{1}{-h} \right\} \phi_1 \left\{ \frac{1}{-h} \right\} = \left\{ \frac{1}{ae^{i\theta}} \right\} R\delta, \tag{3.8}$$

$$\delta = -\frac{i\alpha}{R^2} (i\alpha R d + \alpha^2 R^2 m - \alpha^4 B - \alpha^2 T - K), \tag{3.9}$$

8 Effect of wall compliance on peristaltic transport

$$\phi_{20}''''(y) = -\frac{i\alpha R}{2}(\phi_1(y)\phi_1''^*(y) - \phi_1^*(y)\phi_1''(y))', \quad (3.10)$$

$$\phi_{20}' \left\{ \begin{matrix} 1 \\ -h \end{matrix} \right\} \pm \frac{1}{2} \left\{ \begin{matrix} 1 \\ 2a \cos \theta \end{matrix} \right\} \left(\phi_1' \left\{ \begin{matrix} 1 \\ -h \end{matrix} \right\} + \phi_1''^* \left\{ \begin{matrix} 1 \\ -h \end{matrix} \right\} \right) = -\frac{1}{2} \left\{ \begin{matrix} 1 \\ a^2 \end{matrix} \right\} \psi_0'''' \left\{ \begin{matrix} 1 \\ -h \end{matrix} \right\}, \quad (3.11)$$

$$\begin{aligned} \phi_{20}'''' \left\{ \begin{matrix} 1 \\ -h \end{matrix} \right\} &= -\frac{i\alpha R}{2} \left(\phi_1 \left\{ \begin{matrix} 1 \\ -h \end{matrix} \right\} \phi_1''^* \left\{ \begin{matrix} 1 \\ -h \end{matrix} \right\} - \phi_1^* \left\{ \begin{matrix} 1 \\ -h \end{matrix} \right\} \phi_1'' \left\{ \begin{matrix} 1 \\ -h \end{matrix} \right\} \right) \\ &\mp \frac{1}{2} \left\{ \begin{matrix} 1 \\ ae^{i\theta} \end{matrix} \right\} \left(\phi_1''''^* \left\{ \begin{matrix} 1 \\ -h \end{matrix} \right\} - \alpha(\alpha + iR)\phi_1''^* \left\{ \begin{matrix} 1 \\ -h \end{matrix} \right\} - i\alpha R\phi_1^* \left\{ \begin{matrix} 1 \\ -h \end{matrix} \right\} \psi_0'''' \left\{ \begin{matrix} 1 \\ -h \end{matrix} \right\} \right) \\ &\mp \frac{1}{2} \left\{ \begin{matrix} 1 \\ ae^{-i\theta} \end{matrix} \right\} \left(\phi_1'''' \left\{ \begin{matrix} 1 \\ -h \end{matrix} \right\} - \alpha(\alpha - iR)\phi_1'' \left\{ \begin{matrix} 1 \\ -h \end{matrix} \right\} + i\alpha R\phi_1 \left\{ \begin{matrix} 1 \\ -h \end{matrix} \right\} \psi_0'''' \left\{ \begin{matrix} 1 \\ -h \end{matrix} \right\} \right), \end{aligned} \quad (3.12)$$

$$\begin{aligned} &\left(\frac{d^2}{dy^2} - 4\alpha^2 + 2i\alpha R \right) \left(\frac{d^2}{dy^2} - 4\alpha^2 \right) \phi_{22}(y) \\ &= 2i\alpha R \psi_0' \left(\frac{d^2}{dy^2} - 4\alpha^2 \right) \phi_{22}(y) - 2i\alpha R \psi_0'''' \phi_{22}(y) + \frac{i\alpha R}{2} (\phi_1'(y)\phi_1''(y) - \phi_1(y)\phi_1'''(y)), \end{aligned}$$

$$\phi_{22}' \left\{ \begin{matrix} 1 \\ -h \end{matrix} \right\} = -\frac{1}{4} \left\{ \begin{matrix} 1 \\ a^2 e^{2i\theta} \end{matrix} \right\} \psi_0'''' \left\{ \begin{matrix} 1 \\ -h \end{matrix} \right\} \mp \frac{1}{2} \left\{ \begin{matrix} 1 \\ ae^{i\theta} \end{matrix} \right\} \phi_1'' \left\{ \begin{matrix} 1 \\ -h \end{matrix} \right\},$$

$$\begin{aligned} 2\phi_{22}'''' \left\{ \begin{matrix} 1 \\ -h \end{matrix} \right\} &= 4\alpha(2\alpha - iR)\phi_{22}' \left\{ \begin{matrix} 1 \\ -h \end{matrix} \right\} + i\alpha R\phi_1'^2 \left\{ \begin{matrix} 1 \\ -h \end{matrix} \right\} - i\alpha R\phi_1 \left\{ \begin{matrix} 1 \\ -h \end{matrix} \right\} \phi_1'' \left\{ \begin{matrix} 1 \\ -h \end{matrix} \right\} \\ &\mp \left\{ \begin{matrix} 1 \\ ae^{i\theta} \end{matrix} \right\} \left(\phi_1''''^* \left\{ \begin{matrix} 1 \\ -h \end{matrix} \right\} + \alpha(iR - \alpha)\phi_1''^* \left\{ \begin{matrix} 1 \\ -h \end{matrix} \right\} + i\alpha R\psi_0'''' \left\{ \begin{matrix} 1 \\ -h \end{matrix} \right\} \phi_1 \left\{ \begin{matrix} 1 \\ -h \end{matrix} \right\} \right) \\ &- 4i\alpha R\psi_0'' \left\{ \begin{matrix} 1 \\ -h \end{matrix} \right\} \phi_{22} \left\{ \begin{matrix} 1 \\ -h \end{matrix} \right\}, \end{aligned} \quad (3.13)$$

where (') denotes the derivative with respect to y . These equations are sufficient to determine the solution up to the second order in ϵ . But these equations are fourth-order ordinary differential equations with variable coefficients, the boundary conditions are not all homogeneous, and the problem is not an eigenvalue problem. However, we can restrict our investigation to the case of free-pumping. Physically, this means that the fluid is stationary if there is no peristaltic waves. In this case we put $(\partial p / \partial x)_0 = 0$ which means $K_0 = 0$, under this assumption we get a solution of (3.6) in the form

$$\phi_1(y) = L1 \sinh \alpha y + L2 \cosh \alpha y + L3 \sinh \beta y + L4 \cosh \beta y, \quad (3.14)$$

where

$$\begin{aligned}
 L1 &= \frac{-(\alpha L2 \operatorname{Sinh} \alpha + \beta L3 \operatorname{Cosh} \beta + \beta L4 \operatorname{Sinh} \beta)}{\alpha \operatorname{Cosh} \alpha}, \\
 L2 &= \frac{-(N3R\delta + N5N9L3)}{N1N5}, \\
 L3 &= \frac{R\delta(N1N8 - N3N6 - aN1N5e^{i\theta})}{N5(N6N9 - N1N10)}, \\
 L4 &= \frac{-(N1L2 + N2L3)}{N3}, \\
 N1 &= \frac{\alpha(\operatorname{Cosh} ah \operatorname{Sinh} \alpha + \operatorname{Cosh} \alpha \operatorname{Sinh} ah)}{\operatorname{Cosh} \alpha}, \\
 N2 &= \frac{\beta(\operatorname{Cosh} ah \operatorname{Cosh} \beta - \operatorname{Cosh} \beta h \operatorname{Cosh} \alpha)}{\operatorname{Cosh} \alpha}, \\
 N3 &= \frac{\beta(\operatorname{Cosh} ah \operatorname{Sinh} \beta + \operatorname{Sinh} \beta h \operatorname{Cosh} \alpha)}{\operatorname{Cosh} \alpha}, \\
 N4 &= \beta(\beta^2 - \alpha^2) \operatorname{Cosh} \beta, \quad N5 = \beta(\beta^2 - \alpha^2) \operatorname{Sinh} \beta, \\
 N6 &= \frac{-i\alpha^2 R(\operatorname{Cosh} ah \operatorname{Sinh} \alpha + \operatorname{Cosh} \alpha \operatorname{Sinh} ah)}{\operatorname{Cosh} \alpha}, \\
 N7 &= \frac{\beta((\beta^2 - \alpha(\alpha - iR)) \operatorname{Cosh} \alpha \operatorname{Cosh} \beta h - i\alpha R \operatorname{Cosh} ah \operatorname{Cosh} \beta)}{\operatorname{Cosh} \alpha}, \\
 N8 &= \frac{-\beta((\beta^2 - \alpha(\alpha - iR)) \operatorname{Cosh} \alpha \operatorname{Sinh} \beta h + i\alpha R \operatorname{Cosh} ah \operatorname{Sinh} \beta)}{\operatorname{Cosh} \alpha}, \\
 N9 &= \frac{(N5N2 - N3N4)}{N5}, \quad N10 = \frac{(N5N7 - N4N8)}{N5}, \\
 \beta^2 &= \alpha^2 - i\alpha R.
 \end{aligned} \tag{3.15}$$

Next, in the expansion of ψ_2 , we need only to concern ourselves with the terms $\phi'_{20}(y)$ as our aim is to determine the mean flow only. Thus, the solution of the differential equation (3.10) subject to boundary conditions (3.11) and (3.12), under the assumption that $K_0 = 0$, gives the expression

$$\phi'_{20}(y) = F(y) + g(y) + c_1 y^2 + c_2 y + c_3. \tag{3.16}$$

Thus, the peristaltic mean flow is obtained as

$$\bar{u}(y) = \frac{\epsilon^2}{2} \phi'_{20}(y) = \frac{\epsilon^2}{2} (F(y) + g(y) + c_1 y^2 + c_2 y + c_3), \tag{3.17}$$

10 Effect of wall compliance on peristaltic transport

$$\begin{aligned}
 c_1 &= \frac{(D3 - s)}{2}, \\
 c_2 &= \frac{(2(D1 - F(1)) - 2(D2 - F(-h)) - 2g(1) + 2g(-h) - (1 - h^2)(D3 - s))}{2(1 + h)}, \\
 c_3 &= \frac{(2h(D1 - F(1)) + 2(D2 - F(-h)) + 2g(-h) - 2hg(1) - h(1 + h)(D3 - s))}{2(1 + h)}, \\
 D1 &= \frac{-1}{2} (\alpha^2(L1 + L1^*) \text{Sinh } \alpha + \alpha^2(L2 + L2^*) \text{Cosh } \alpha + \beta^2 L3 \text{Sinh } \beta + \beta^2 L4 \text{Cosh } \beta \\
 &\quad + \beta^{*2} L3^* \text{Sinh } \beta^* + \beta^{*2} L4^* \text{Cosh } \beta^*), \\
 D2 &= -a \text{Cos } \theta (\alpha^2(L1 + L1^*) \text{Sinh } \alpha h - \alpha^2(L2 + L2^*) \text{Cosh } \alpha h + \beta^2 L3 \text{Sinh } \beta h \\
 &\quad - \beta^2 L4 \text{Cosh } \beta h + \beta^{*2} L3^* \text{Sinh } \beta^* h - \beta^{*2} L4^* \text{Cosh } \beta^* h), \\
 D3 &= \frac{-i\alpha R}{2} ((\beta^{*2} - \alpha^2)(L1L3^* \text{Sinh } \alpha \text{Sinh } \beta^* + L1L4^* \text{Sinh } \alpha \text{Cosh } \beta^*) \\
 &\quad + (\beta^{*2} - \alpha^2)(L2L3^* \text{Cosh } \alpha \text{Sinh } \beta^* + L2L4^* \text{Cosh } \alpha \text{Cosh } \beta^*) \\
 &\quad + (\alpha^2 - \beta^2)(L3L1^* \text{Sinh } \alpha \text{Sinh } \beta + L4L1^* \text{Sinh } \alpha \text{Cosh } \beta) \\
 &\quad + (\alpha^2 - \beta^2)(L3L2^* \text{Cosh } \alpha \text{Sinh } \beta + L4L2^* \text{Cosh } \alpha \text{Cosh } \beta) \\
 &\quad + (\beta^{*2} - \beta^2)(L3L3^* \text{Sinh } \beta \text{Sinh } \beta^* + L3L4^* \text{Sinh } \beta \text{Cosh } \beta^*) \\
 &\quad + (\beta^{*2} - \beta^2)(L4L3^* \text{Cosh } \beta \text{Sinh } \beta^* + L4L4^* \text{Cosh } \beta \text{Cosh } \beta^*)) \\
 &\quad - \frac{1}{2} ((\alpha^4(L1 + L1^*) - \alpha^3(\alpha + iR)L1^* - \alpha^3(\alpha - iR)L1) \text{Sinh } \alpha \\
 &\quad + (\alpha^4(L2 + L2^*) - \alpha^3(\alpha + iR)L2^* - \alpha^3(\alpha - iR)L2) \text{Cosh } \alpha \\
 &\quad + (\beta^{*4} - \alpha\beta^{*2}(\alpha + iR))L3^* \text{Sinh } \beta^* + (\beta^{*4} - \alpha\beta^{*2}(\alpha + iR))L4^* \text{Cosh } \beta^* \\
 &\quad + (\beta^4 - \alpha\beta^2(\alpha - iR))L3 \text{Sinh } \beta + (\beta^4 - \alpha\beta^2(\alpha - iR))L4 \text{Cosh } \beta), \\
 s &= \frac{-i\alpha R}{4} ((\beta^{*2} - \alpha^2)(L1L3^* + L2L4^*) \text{Cosh } (\alpha + \beta^*) \\
 &\quad - (\beta^{*2} - \alpha^2)(L1L3^* - L2L4^*) \text{Cosh } (\alpha - \beta^*) \\
 &\quad + (\alpha^2 - \beta^2)(L3L1^* + L4L2^*) \text{Cosh } (\alpha + \beta) \\
 &\quad - (\alpha^2 - \beta^2)(L3L1^* - L4L2^*) \text{Cosh } (\alpha - \beta) \\
 &\quad + (\beta^{*2} - \beta^2)(L3L3^* + L4L4^*) \text{Cosh } (\beta + \beta^*) \\
 &\quad - (\beta^{*2} - \beta^2)(L3L3^* - L4L4^*) \text{Cosh } (\beta - \beta^*) \\
 &\quad + (\beta^{*2} - \alpha^2)(L1L4^* + L2L3^*) \text{Sinh } (\beta^* + \alpha) \\
 &\quad - (\beta^{*2} - \alpha^2)(L1L4^* - L2L3^*) \text{Sinh } (\beta^* - \alpha) \\
 &\quad + (\alpha^2 - \beta^2)(L3L2^* + L4L1^*) \text{Sinh } (\alpha + \beta) \\
 &\quad - (\alpha^2 - \beta^2)(L3L2^* - L4L1^*) \text{Sinh } (\alpha - \beta) \\
 &\quad + (\beta^{*2} - \beta^2)(L3L4^* + L4L3^*) \text{Sinh } (\beta^* + \beta) \\
 &\quad - (\beta^{*2} - \beta^2)(L3L4^* - L4L3^*) \text{Sinh } (\beta^* - \beta)),
 \end{aligned}$$

(3.18)

$$\begin{aligned}
F(y) = & \frac{-i\alpha R}{4} \left(\frac{(\beta^{*2} - \alpha^2)(L1L3^* + L2L4^*)}{(\alpha + \beta^*)^2} \text{Cosh}(\alpha + \beta^*)y \right. \\
& - \frac{(L1L3^* - L2L4^*)}{(\alpha - \beta^*)^2} \times (\beta^{*2} - \alpha^2) \text{Cosh}(\alpha - \beta^*)y \\
& + \frac{(\alpha^2 - \beta^2)(L3L1^* + L4L2^*)}{(\alpha + \beta)^2} \text{Cosh}(\alpha + \beta)y \\
& - \frac{(\alpha^2 - \beta^2)(L3L1^* - L4L2^*)}{(\alpha - \beta)^2} \text{Cosh}(\alpha - \beta)y + \frac{(L3L3^* + L4L4^*)}{(\beta + \beta^*)^2} \\
& \times (\beta^{*2} - \beta^2) \text{Cosh}(\beta + \beta^*)y - \left. \frac{(\beta^{*2} - \beta^2)(L3L3^* - L4L4^*)}{(\beta - \beta^*)^2} \text{Cosh}(\beta - \beta^*)y \right), \\
g(y) = & \frac{-i\alpha R}{4} \left(\frac{(\beta^{*2} - \alpha^2)(L1L4^* + L2L3^*)}{(\alpha + \beta^*)^2} \text{Sinh}(\alpha + \beta^*)y + \frac{(L1L4^* - L2L3^*)}{(\alpha - \beta^*)^2} \right. \\
& \times (\beta^{*2} - \alpha^2) \text{Sinh}(\alpha - \beta^*)y + \frac{(\alpha^2 - \beta^2)(L3L2^* + L4L1^*)}{(\alpha + \beta)^2} \text{Sinh}(\alpha + \beta)y \\
& - \frac{(\alpha^2 - \beta^2)(L3L2^* - L4L1^*)}{(\alpha - \beta)^2} \text{Sinh}(\alpha - \beta)y + \frac{(L3L4^* + L4L3^*)}{(\beta + \beta^*)^2} \\
& \times (\beta^{*2} - \beta^2) \text{Sinh}(\beta + \beta^*)y + \left. \frac{(\beta^{*2} - \beta^2)(L3L4^* - L4L3^*)}{(\beta - \beta^*)^2} \text{Sinh}(\beta - \beta^*)y \right).
\end{aligned} \tag{3.19}$$

The last solution (3.17) differs with that of Fung and Yih [10] in many respects. Interestingly enough, when the equation of motion of the wall is satisfied, c_1 is determined completely. In the cited reference, c_1 remained arbitrary and its determination was attributed to the considerations of conditions at the ends of the channel. It should be noted that if we put $a = h = 1$, $\theta = 0$, and the wall parameters tend to zero, then the results of the problem reduce exactly to the same as that found by Fung and Yih [10]. Also, if we put $a = h = 1$, $\theta = 0$, and wall tension T and wall elastance $K \rightarrow 0$ (thin plate) and wall rigidity B and wall elastance $K \rightarrow 0$ (membrane), then the results of the problem agree with the work of Mitra and Prasad [17].

4. Numerical results and discussion

In order to observe the quantitative effects of various parameters involved in the analysis, the mean velocity at the boundaries of the channel, the time-averaged mean-axial velocity distribution, and reversal flow are calculated for various values of these parameters. Computer codes were developed for the numerical evaluations of the analytical results and some important results are displayed graphically in Figures 4.1–4.10. The constant $D1$, which initially arose from the nonslip condition of the axial velocity on the upper wall, is due to the value of ϕ'_{20} at the upper wall and is related to the mean velocity by

12 Effect of wall compliance on peristaltic transport

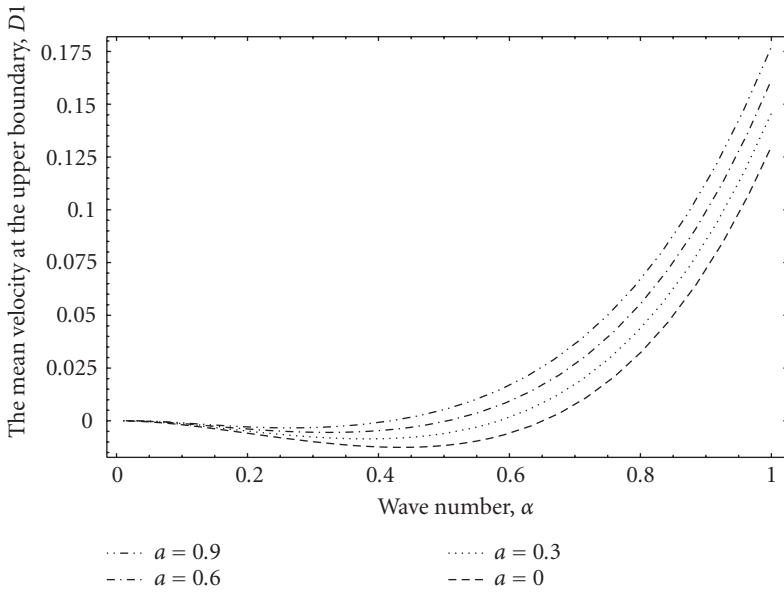


Figure 4.1. Effect of the wave amplitude ratio a on variation of $D1$ with wave number α for $m = 0.01$, $B = 20$, $T = 10$, $K = 10$, $d = 0.5$, $h = 0.5$, $\theta = \pi/3$, and $R = 15$.

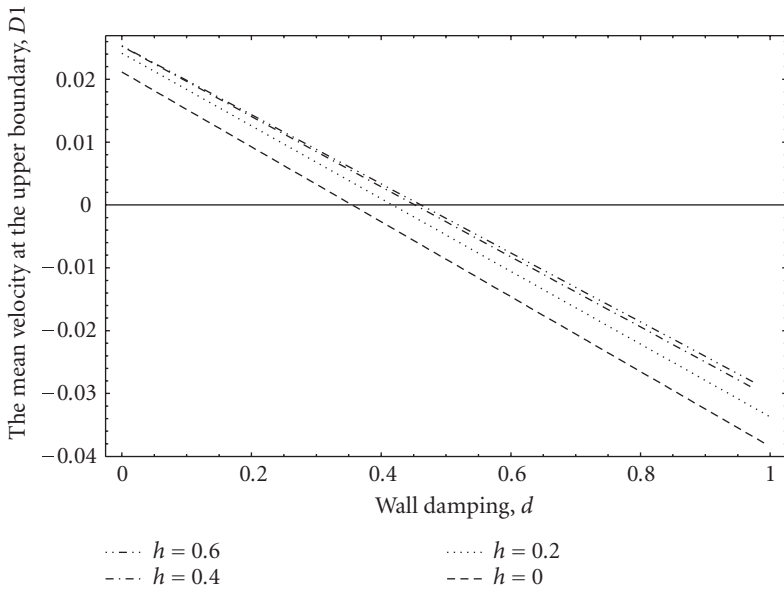


Figure 4.2. Effect of the width of the channel h on variation of $D1$ with wall damping d for $m = 0.01$, $B = 20$, $T = 10$, $K = 10$, $\alpha = 0.5$, $a = 0.5$, $\theta = \pi/3$, and $R = 15$.

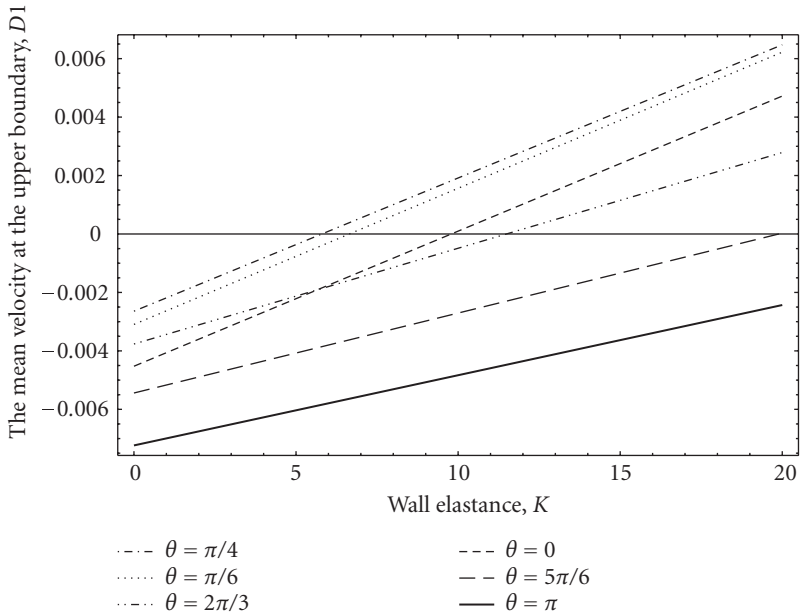


Figure 4.3. Effect of the phase difference θ on variation of $D1$ with wall elastance K for $m = 0.01$, $B = 10$, $T = 5$, $d = 0.2$, $\alpha = 0.5$, $a = 0.5$, $h = 0.5$, and $R = 15$.

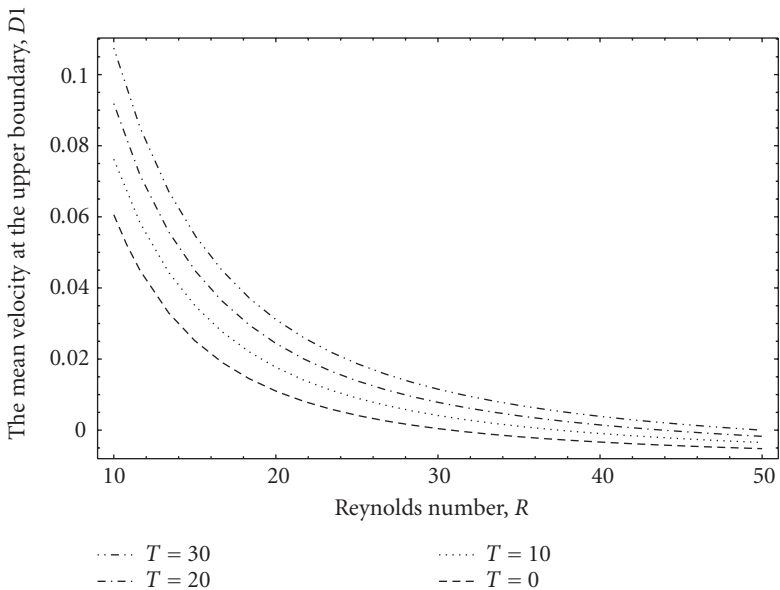


Figure 4.4. Effect of the wall tension T on variation of $D1$ with Reynolds number R for $m = 0.01$, $B = 100$, $d = 0.2$, $\theta = \pi/6$, $\alpha = 0.4$, $a = 0.5$, $h = 0.5$, and $K = 50$.

14 Effect of wall compliance on peristaltic transport

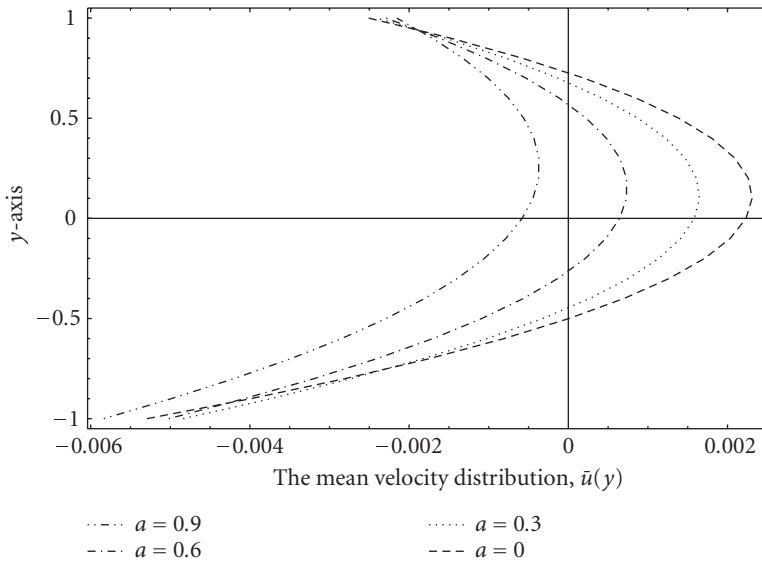


Figure 4.5. Effect of the wave amplitude ratio a on the mean-velocity distribution and reversal flow for $m = 0.01, B = 20, T = 10, K = 10, d = 0.5, h = 0.5, \theta = \pi/3, \epsilon = 0.5, \alpha = 0.5,$ and $R = 50$.

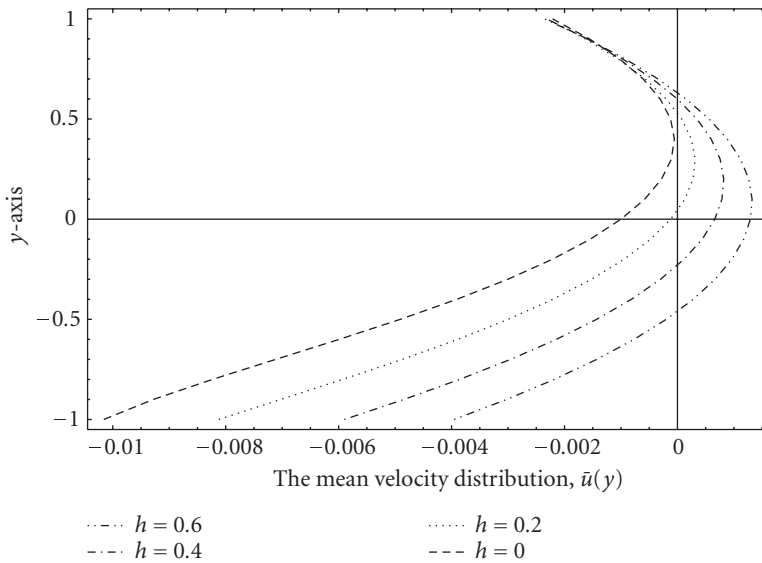


Figure 4.6. Effect of the width of the channel h on the mean-velocity distribution and reversal flow for $m = 0.01, B = 20, T = 10, K = 10, d = 0.5, a = 0.5, \theta = \pi/3, \epsilon = 0.5, \alpha = 0.5,$ and $R = 50$.

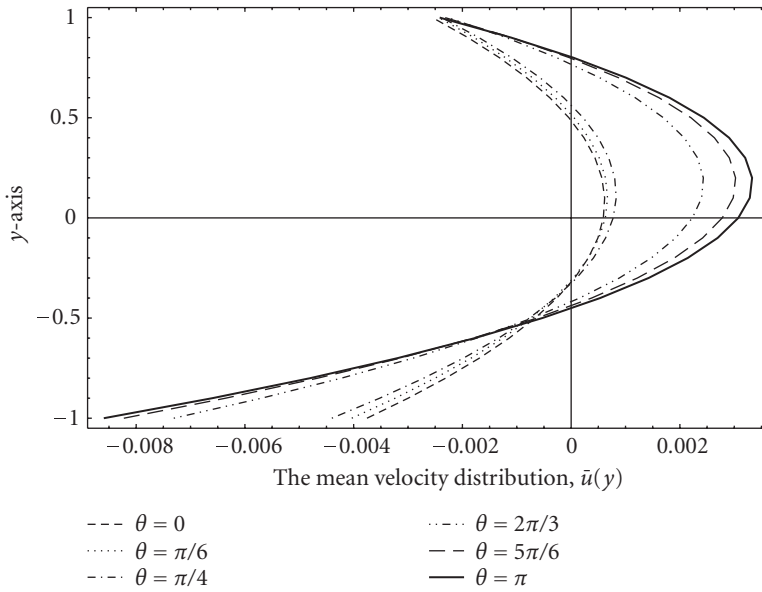


Figure 4.7. Effect of the phase difference θ on the mean-velocity distribution and reversal flow for $m = 0.01, B = 20, T = 10, K = 10, d = 0.5, a = 0.5, h = 0.5, \epsilon = 0.5, \alpha = 0.5,$ and $R = 50$.

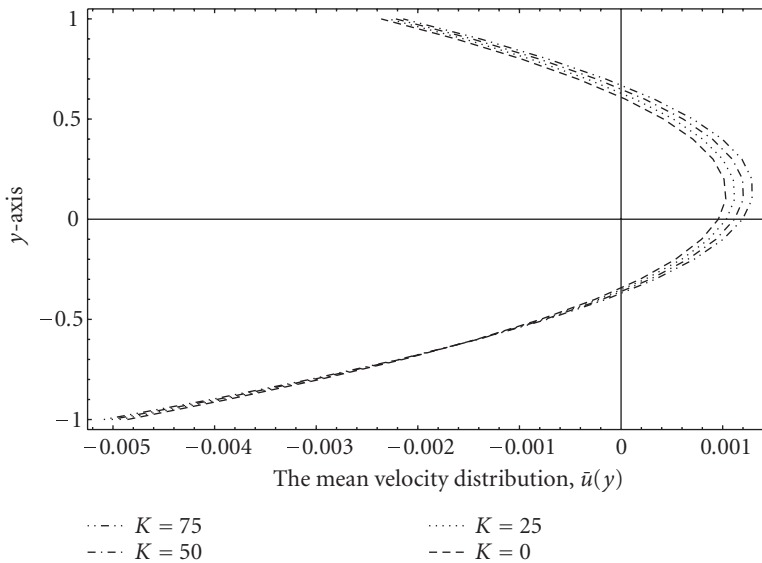


Figure 4.8. Effect of the wall elastance K on the mean-velocity distribution and reversal flow for $m = 0.01, B = 20, T = 10, \theta = \pi/3, d = 0.5, a = 0.5, h = 0.5, \epsilon = 0.5, \alpha = 0.5,$ and $R = 50$.

16 Effect of wall compliance on peristaltic transport

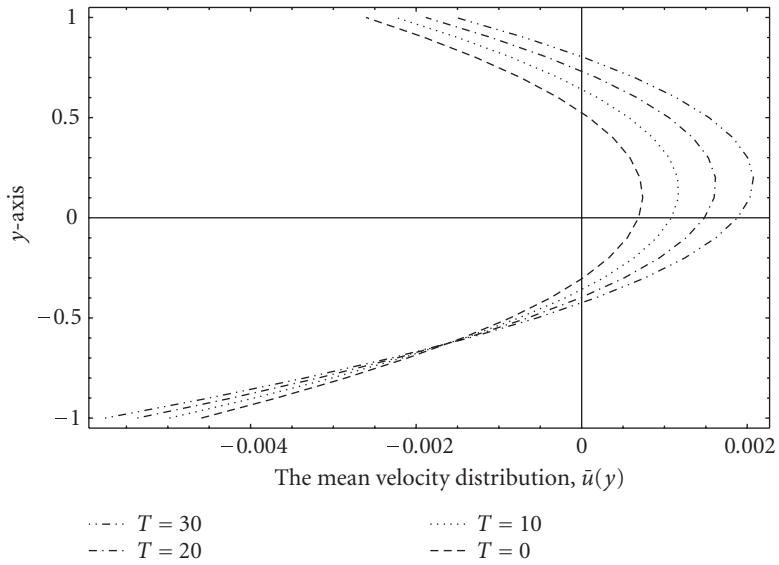


Figure 4.9. Effect of the wall tension T on the mean-velocity distribution and reversal flow for $m = 0.01, B = 20, d = 0.5, \theta = \pi/3, K = 40, a = 0.5, h = 0.5, \epsilon = 0.5, \alpha = 0.5,$ and $R = 50$.

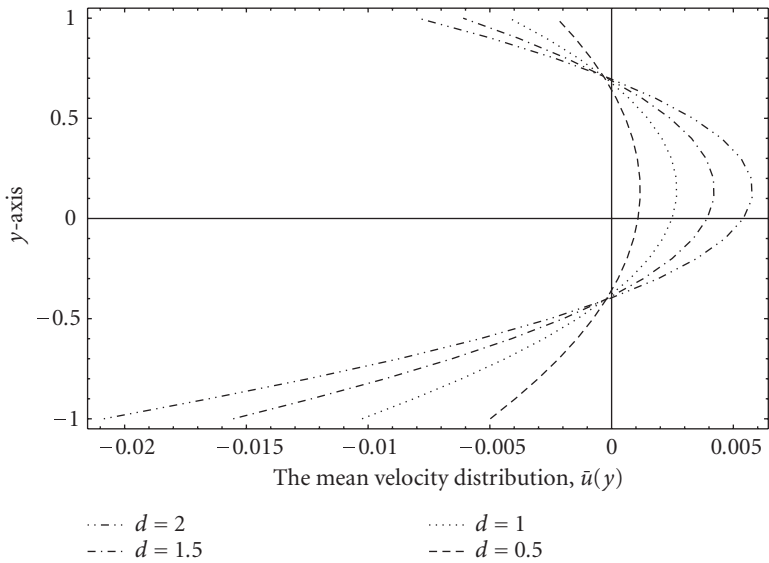


Figure 4.10. Effect of the wall damping d on the mean-velocity distribution and reversal flow for $m = 0.01, B = 20, T = 10, \theta = \pi/3, K = 40, a = 0.5, h = 0.5, \epsilon = 0.5, \alpha = 0.5,$ and $R = 50$.

$\bar{u}(1) = (\epsilon^2/2)\phi'_{20}(1) = (\epsilon^2/2)D1$. The variation of the mean velocity at the upper boundary $D1$ with the wave number α is presented in Figure 4.1 for different values of wave amplitude ratio a . It is observed that $D1$ increases with the increasing of a . Further, it is easy to observe that $D1$ decreases for some α small in the beginning but it starts increasing for α large as the Poiseuille flow due to pressure loss dominates the peristaltic flow. Figure 4.2 shows the variation of $D1$ with the wall damping d for different values of the width of the channel h . It shows that $D1$ increases with the increasing of h , and little differences are seen at large values of h . Also, we observe that $D1$ decreases as d increases, becomes zero for some d , and remains negative afterwards until d becomes 1, indicating that damping may cause the mean flow reversal at the walls, which is not possible in the elastic symmetric channel case. Figure 4.3 depicts the variation of $D1$ with the wall elastance K for different values of phase difference θ . It is observed that by the increasing of θ , $D1$ increases for all $0 \leq \theta \leq \pi/2$ and decreases for all $\pi/2 < \theta \leq \pi$. Also, we show that $D1$ increases with the increasing of K . The effect of the wall tension T on the variation of $D1$ with the Reynolds number R is depicted in Figure 4.4. It is observed that $D1$ increases with the increasing of T and it decreases with the increasing of R . Yin and Fung [27] define a flow reflux whenever there is a negative-mean velocity in the flow field. The effects of wave amplitude ratio a , width of the channel h , phase difference θ , wall elastance K , wall tension T , and wall damping d on mean-velocity and reversal flow are displayed in Figures 4.5–4.10. The results reveal that the reversal flow occurs near the boundaries where the direction of the velocity changes from positive to negative. Further, it can be shown that the reversal flow near the upper wall is much less than that near the lower wall. A comparison of the results with those for symmetric channel reveals that the curves do shift towards the upper wall in an asymmetric channel, whereas in a symmetric channel these are symmetric about the center line of the channel. As shown in Figures 4.5 and 4.6, in the narrow part of the channel near the upper wall, the possibility of flow reversal decreases by the increasing of a and increases with the increasing of h . While in the remaining wide part of the channel, the possibility of flow reversal increases by the increasing of a and decreases with the increasing of h . It is also seen from Figures 4.7–4.9 that, in the narrow part of the channel near the upper wall, the possibility of flow reversal increases by the increasing of θ , K , and T . While in the remaining wide part of the channel, the possibility of flow decreases with the increasing of θ , K , and T . Finally, from Figure 4.10 it is noticed that, near the boundaries of the channel, the possibility of flow reversal increases by the increasing of d , while in the remaining wide part of the channel, the possibility of flow decreases with increasing d .

References

- [1] C. Barton and S. Raynor, *Peristaltic flow in tubes*, Bulletin of Mathematical Biophysics **30** (1968), 663–680.
- [2] T. D. Brown and T. K. Hung, *Computational and experimental investigations of two-dimensional nonlinear peristaltic flows*, Journal of Fluid Mechanics **83** (1977), 249–272.
- [3] J. C. Burns and T. Parkes, *Peristaltic motion*, Journal of Fluid Mechanics **29** (1967), 731–743.
- [4] C. Davies and P. W. Carpenter, *Instabilities in a plane channel flow between compliant walls*, Journal of Fluid Mechanics **352** (1997), 205–243.

- [5] K. de Vries, E. A. Lyons, J. Ballard, C. S. Levi, and D. J. Lindsay, *Contractions of the inner third of the myometrium*, American Journal of Obstetrics and Gynecology **162** (1990), no. 3, 679–682.
- [6] E. C. Eckstein, *Experimental and theoretical pressure studies of peristaltic pumping*, Master's thesis, MIT, Massachusetts, 1970.
- [7] E. F. El-Shehawey and Kh. S. Mekheimer, *Couple-stresses in peristaltic transport of fluids*, Journal of Physics D: Applied Physics **27** (1994), no. 6, 1163–1170.
- [8] O. Eytan and D. Elad, *Analysis of intra-uterine fluid motion induced by uterine contractions*, Bulletin of Mathematical Biology **61** (1999), no. 2, 221–238.
- [9] O. Eytan, A. J. Jaffa, J. Har-Toov, E. Dalach, and D. Elad, *Dynamics of the intrauterine fluid-wall interface*, Annals of Biomedical Engineering **27** (1999), no. 3, 372–379.
- [10] Y. C. Fung and C. S. Yih, *Peristaltic transport*, ASME Transactions: Journal of Applied Mechanics **35** (1968), 669–675.
- [11] M. H. Haroun, *Effect of relaxation and retardation time on peristaltic transport of the Oldroydian viscoelastic fluid*, Journal of Applied Mechanics and Technical Physics **46** (2005), no. 6, 842–850.
- [12] T. W. Latham, *Fluid motion in a peristaltic pump*, Master's thesis, MIT, Massachusetts, 1966.
- [13] Kh. S. Mekheimer, *Peristaltic transport of a couple-stress fluid in a uniform and non-uniform channels*, Biorheology **39** (2002), no. 6, 755–765.
- [14] ———, *Nonlinear peristaltic transport through a porous medium in an inclined planar channel*, Journal of Porous Media **6** (2003), no. 3, 189–201.
- [15] Kh. S. Mekheimer, E. F. El-Shehawey, and A. M. Elaw, *Peristaltic motion of a particle-fluid suspension in a planar channel*, International Journal of Theoretical Physics **37** (1998), no. 11, 2895–2920.
- [16] M. Mishra and A. R. Rao, *Peristaltic transport of a Newtonian fluid in an asymmetric channel*, Zeitschrift für angewandte Mathematik und Physik **54** (2003), no. 3, 532–550.
- [17] T. K. Mitra and S. N. Prasad, *On the influence of wall properties and Poiseuille flow in peristalsis*, Journal of Biomechanics **6** (1973), no. 6, 681–693.
- [18] S. K. Paufler and R. H. Foote, *Morphology motility and fertility of spermatozoa recovered from different areas of ligated rabbit epididymides*, Journal of Reproduction and Fertility **17** (1968), 125–137.
- [19] A. H. Shapiro, M. Y. Jaffrin, and S. L. Weinberg, *Peristaltic pumping with long wave lengths at low Reynolds number*, Journal of Fluid Mechanics **37** (1969), no. 4, 799–825.
- [20] V. P. Srivastava and M. Saxena, *A two-fluid model of non-Newtonian blood flow induced by peristaltic waves*, Rheologica Acta **34** (1995), no. 4, 406–414.
- [21] L. M. Srivastava and V. P. Srivastava, *Peristaltic transport of blood: Casson model—II*, Journal of Biomechanics **17** (1984), no. 11, 821–829.
- [22] ———, *Peristaltic transport of a particle-fluid suspension*, Journal of Biomechanical Engineering **111** (1989), no. 2, 157–165.
- [23] S. Takabatake and K. Ayukawa, *Numerical study of two-dimensional peristaltic flows*, Journal of Fluid Mechanics **122** (1982), 439–465.
- [24] S. Takabatake, K. Ayukawa, and A. Mori, *Peristaltic pumping in circular cylindrical tubes: a numerical study of fluid transport and its efficiency*, Journal of Fluid Mechanics **193** (1988), 267–283.
- [25] S. L. Weinberg, *A theoretical and experimental treatment of peristaltic pumping and its relation to ureteral function*, Ph.D. thesis, MIT, Massachusetts, 1970.

- [26] S. L. Weinberg, E. C. Eckstein, and A. H. Shapiro, *An experimental study of peristaltic pumping*, Journal of Fluid Mechanics **49** (1971), 461–497.
- [27] C. C. Yin and Y. C. Fung, *Peristaltic waves in circular cylindrical tubes*, Journal of Applied Mechanics **36** (1969), 579–587.

Mohamed H. Haroun: Department of Mathematics, Girls College of Education,
Qassim El-Mezneb, Saudi Arabia
E-mail address: hassan6aky@yahoo.com



Hindawi

Submit your manuscripts at
<http://www.hindawi.com>

